Amendment to Page 1 of

SEMI-ANNUAL TECHNICAL REPORT
January 1st - June 30th, 1971

ARPA ORDER NUMBER 1482 Amdt 2
PROGRAM CODE NUMBER 0E20

Name of Grantee
COLUMBIA UNIVERSITY
NEW YORK, NEW YORK

Effective Date of Grant
30 JUNE 1970

Grant Number
DA-ARO-D-31-124-70-G103

Amount of Grant: $50,000

Principal Investigator
Professor Richard N. Zare
(212) 280-2017

Short Title of Work
METAL OXIDE INFRARED EMISSION

Sponsored by
ADVANCED RESEARCH PROJECTS AGENCY
ARPA ORDER NUMBER 1482 Amdt 2

TABLE OF CONTENTS

PROGRESS AT LARGE

The AVCO Dial-A-Line dye laser has been installed and is in working order. The Fabry-Perot etalon arrived the last weeks in June and permits the laser output to be narrowed to 1 Å or less. Dr. Irving Itskin of AVCO has demonstrated the expected narrowing in our laboratory. We have immediate plans to use this for laser-induced fluorescence studies of metal oxides. We will attempt to obtain lifetime data by observing the fluorescence decay on a fast oscilloscope.

During this period we set up a Welsbach ozonator to study metal atom reactions with ozone. Of particular interest to us was the reaction $Ba + O_3 \rightarrow BaO^* + O_2$. The chemiluminescence is identical in features but different in intensity compared to the reaction $Ba + N_2O \rightarrow BaO^* + N_2$. The latter (see below) has been tentatively assigned to a triplet metal oxide emitter. The fact that $Ba + N_2O$ and $Ba + O_3$ yield the same emitter is further evidence that

we are observing a heretofore unidentified band system of BaO. Ozone reactions with other metal systems are now in progress.

In addition, our studies of two-body radiative recombination are being continued. A systematic investigation is being made of the reactions $M + X_2$ or $XY \rightarrow MX_2$ or MXY where M = Ba, Sr, Ca, and Mg, and X_2 or XY = Cl_2, Br_2, I_2, ICl, IBr. All reactions show the characteristic two-body radiative recombination continuum reported in the April issue of Chem. Phys. Letters 9, 65 (1971).

The following manuscript on "Crossed-Beam Chemiluminescence Studies of Some Group IIA Metal Oxides," which has been submitted for publication as an article to The Journal of Chemical Physics by C. D. Jonah, R. N. Zare, and Ch. Ottinger, resulted from much of the work during the past six months. Support was furnished by the U. S. Army under Grant DA-ARO-D-31-124-70-G55 in addition to that provided by ARPA.

SUMMARY

Chemiluminescence from a beam of group IIA metals traversing a scattering chamber filled with NO_2 or N_2O gas has been studied as a function of wavelength and pressure. The Ba + NO_2 and the Ba, Sr, and Ca + N_2O chemiluminescent reactions are first order in both reactants while Ca + NO_2 and Sr + NO_2 are quadratic in the NO_2 pressure. Cross sections for beam attenuation are about 90 to 170 $Å^2$ for reactions with NO_2 (consistent with an electron-jump model), while those for N_2O are 15 to 30 $Å^2$. For the Ba + NO_2 reaction, the chemiluminescence has been assigned to the BaO $A\,^1\Sigma - X\,^1\Sigma$ band system. From the resolved rotational structure it is concluded that with higher v' excitation, the J' distribution is characterized by a lower rotational temperature. A lower bound of 131.5 kcal/mole is placed on D_0°(BaO). For certain reactions the chemiluminescence is weakly polarized. A model involving the partitioning of angular momentum between the rotation and recoil angular momenta of the products is proposed to account for the degree of polarization of the chemiluminescence.

I. INTRODUCTION

Much of the efforts of molecular beamists during the past decade can be likened to reconstructing a "motion picture" of a chemical reaction primarily from angular distribution measurements in order to understand the nature of single reactive collisions. Since the first pioneering experiments[1] more than ten years ago, the field has blossomed rapidly and provided us with much detailed information about the angular distribution of the products, the partitioning of excess chemical energy into translational and all other degrees of freedom, and the variation of the reaction cross section with velocity, impact parameter, and orientation.[2] The specification, as well, of the quantum states of the products certainly would represent an additional important clue to unraveling the reaction dynamics.

However, because molecular beam detectors, such as hot-wire surface ionizers or "universal" mass spectrometers, are fairly insensitive to the internal energy state of the species being detected, it has been difficult to infer the distribution of energy among the various internal degrees

of freedom of the freshly formed products. For certain classes of reactions, crossed-beam studies have yielded information about the rotational or vibrational energy distribution. For highly polar products, it has proved possible in some cases to determine the mean rotational energy by using an inhomogeneous electric two-pole deflection field,[3] the rotational population as a function of J by using an electric quadrupole field,[4] and the vibrational distribution by carrying out molecular beam electric resonance spectroscopy studies.[5] For products with large vibrational energy spacings, it has also proved possible in some cases to determine the vibrational population distribution through an analysis of the product translational energy.[6] Nevertheless, in most crossed-beam experiments performed so far, it has not been possible to deduce the detailed nature of the (v, J) population of the newly formed products.

To increase the number of reactions in which the internal product excitation can be studied, we are attempting to marry the technique of molecular beams with that of molecular spectroscopy. To accomplish this, we have chosen

to study a special class of highly exothermic reactions, namely, those that yield electronically excited products that subsequently fluoresce. By observing the chemiluminescent spectrum of these reactions under single-collision conditions, we hope to discover how the excess energy of reaction is divided among vibrational, rotational, and electronic excitation of the products. The success of this technique presupposes that the emission spectrum can be assigned to the (v', J') levels of the emitter and that vibrational band strengths and rotational line strengths are known or can be calculated, thus permitting the spectral intensity features to be reduced to relative population distributions.

Previously, information on the population of (v, J) levels of newly formed products in chemical reactions has been obtained through infrared chemiluminescence studies, initiated by J. C. Polanyi and co-workers.[7] Because the vibrational lifetimes of the molecular products are typically of the order of 10^{-3} sec or longer, it is necessary to correct the results for the effects of collisional relaxation on the observed population distribution. An-

other consequence of the long vibrational lifetime is that only a small fraction of the excited products are detected. It also should be mentioned that the signal-to-noise problems associated with the use of infrared detectors, which arise particularly with increasing wavelength, have so far limited low pressure infrared emission studies at almost exclusively to products containing hydrogen bonds.

Visible chemiluminescence studies are quite complementary to infrared chemiluminescence studies, since the former do not suffer from some of the disadvantages found in the latter. Because electronic lifetimes are typically of the order of 10^{-6} sec or shorter, collisional degradation of the initial (v', J') population distribution can be neglected at much higher pressures than in infrared chemiluminescence. All excited products will radiate in the field of view of the detector, and moreover, detectors in the visible portion of the spectrum are superior to their counterparts in the infrared. Thus, visible chemiluminescence studies, when applicable, offer a much more sensitive means of detection. It must be stressed, though, that both techniques are "blind" to different types of reactions.

For example, infrared chemiluminescence requires that the vibrationally excited products have an electric dipole moment, and this procedure cannot detect products in the $v = 0$ vibrational level; while visible chemiluminescence studies detect only electronically excited products, and consequently information about "invisible" reactions, such as the formation of vibrationally excited ground-state products, can only be inferred.

The first attempts to observe visible chemiluminescence of molecular species formed under crossed-beam conditions were the efforts of Harrison and Scattergood.[8] They investigated the reactions of O_3 with NO, CO, H_2O, and CS_2 but found no chemiluminescent signal above the "background light" resulting from O_3 reaction on the walls of the vacuum-chamber. About two years later, Ackerman[9] reported detecting visible chemiluminescence from the reaction $O_3 + NO$ in the spectral range 5500 to 8000 Å. He used a combination of broadband interference filters (750-Å FWHM) and different red-sensitive photographic films. The first spectroscopic studies were carried out on the reaction of group IIA metals with various oxidizer gases[10] and with

various halogens.[11] We report here a continuation of the chemiluminescent studies of the group IIA metals with specifically NO_2 and N_2O.

Following the description of the experimental apparatus, we discuss the general features of the chemiluminescent spectra of the group IIA metal reactions with NO_2 and N_2O and suggest some mechanisms to help explain their similarities and differences. Emphasis is placed on total reaction cross sections, electronic states of the species formed, and the (v', J') population distribution of the products. In the final section we report the first observation of polarized emission from crossed-beam chemiluminescence. Measurement of the degree of polarization of the chemiluminescence is shown to be equivalent to a determination of the angular distribution of the emitted light. We present a simple model, based on the division of the total angular moment into rotational (internal) and "recoil" (orbital) angular momenta of the products, which accounts fairly well for our present observations.

II. EXPERIMENTAL PROCEDURE

Experiments are performed with a crossed-beam apparatus named LABSTAR for its ability to obtain the temperatures of late-type stars in the laboratory. Figure 1 shows a schematic diagram of LABSTAR. Basically, the experiments are carried out as follows: A beam of metal atoms effuses from a hot-oven source surrounded by numerous heat shields. This beam then enters a differentially pumped chamber through a 1-cm diameter hole in its bulkhead, where it intersects an uncollimated beam of the oxidizer gas that flows into the reaction chamber through a 0.3-cm diameter orifice. The chemiluminescence is viewed at right angles to both beams through a quartz window mounted on a flange at the side of the reaction chamber.

A. Vacuum System

Attached to the bottom of the oven chamber of LABSTAR is a 4-in. oil diffusion pump (750 liters/sec) with a water-cooled baffle. The reaction chamber of LABSTAR is evacuated

by a 6-in. oil-diffusion pump (1500 liters/sec) without a baffle. In addition, there is a blank flange on the reaction chamber to which another 4-in oil diffusion pump may be attached. Provisions were made for this extra pumping speed so that chemiluminescent reactions with cross sections much less than gas kinetic could be studied at higher gas throughputs. However, this additional pumping speed was unnecessary for the studies reported here.

The diffusion pumps of the oven chamber and the reaction chamber share a common foreline which is evacuated by means of a 1397 Welch forepump (425 liters/min). To avoid attack of the forepump oil by oxidizer gases, particularly NO_2, a demountable liquid-nitrogen-cooled glass trap is inserted in the foreline immediately before the forepump.

The pressure is monitored by two Veeco ionization gauges, one located in the reaction chamber, the other in the oven chamber. With a pressure of 1 millitorr in the reaction chamber, the pressure of the oven chamber is better than 5×10^{-5} torr. Exuberant differential pumping is necessary to maintain a well-defined metal-atom beam as well as to avoid destruction of the hot oven by the oxidizer gases.

B. Metal Source

The metal beam was formed by effusion from a molybdenum oven heated with a three-phase molybdenum-wire resistant winding (50-60-A per leg, ≈ 1 kW total power consumption). A molybdenum heat shield and a water-cooled copper heat shield surround the oven and provide part of the collimation of the beam. The oven is a closed cylinder 10 cm high and 4 cm in diameter. It has a 3-mm hole in the top through which the beam effuses. Occasionally the orifice of the oven clogged when high metal fluxes of Mg, Ca, and Sr were used. This difficulty was never encountered with Ba, which unlike the other group IIA metals is a liquid at the operating temperatures necessary for forming a sufficiently intense beam. Molybdenum was chosen as the oven-wall material because of its resistance to chemical attack by the group IIA metals.

Previously, the metal source in LABSTAR was a crucible placed inside a resistance-heated graphite cylinder.[10] Although this permitted much higher temperatures, the limited capacity of the crucible prevented extended runs.

Magnesium ribbon, calcium turnings, and discs of stron-

tium and barium (cut from a metal bar with a bandsaw) were used as source metals. The metal oxide coating was scraped off, the metal (on the order of a few grams) was placed inside the molybdenum oven, and LABSTAR was pumped down as quickly as possible.

A Granville-Phillips film-thickness monitor (see Fig. 1) was used to measure the beam flux and monitor its long-term stability. Typical beam intensities were in the reaction region 10^{15} atoms/sec.

C. Gas Source

The NO_2 or N_2O gas which was held in a stainless steel ballast tank, was leaked into the system through a micrometer needle valve. The NO_2 and N_2O which are Matheson reagent-grade gases, were used without further purification. Because the gas orifice contains coarse crinkly-foil, there is very little collimation of the gas flow, and consequently the oxidizer gas tends to fill the entire reaction chamber. Occasionally it was useful to be able to switch rapidly between NO_2 and N_2O, which we accomplished by using a second gas ori-

fice in the reaction chamber not shown in Fig. 1.

D. Light Detection System

All spectra were taken in first order with a $\frac{3}{4}$-m Spex 1702 spectrometer with a grating blazed at 5000 Å. An EMI 6256 QA photomultiplier with a "S"(Q) response was used with no cooling, and the current from the photomultiplier was measured with a Keithley 417 picoammeter and a Leeds and Northrup strip-chart recorder. None of the spectra shown in the figures are corrected for the wavelength response of the detection system. One quartz lens was used to gather and focus the chemiluminescence on the entrance slits of the spectrometer.

In addition to spectral studies, the degree of polarization of chemiluminescence was measured. A spinning linear polarizer, shown in Fig. 2, modulated the light at twice the rotation frequency. The magnitude of the ac signal is proportional to $I_{\parallel} - I_{\perp}$, where $I_{\parallel}$ ($I_{\perp}$) refers to the intensity polarized parallel (perpendicular) to the metal beam. The dc signal is proportional to $I_{\parallel} + I_{\perp}$. The degree of polariza-

tion P, defined as

$$P = (I_{\parallel} - I_{\perp})/(I_{\parallel} + I_{\perp}) \ , \qquad (1)$$

is obtained directly by feeding the ac signal through a lock-in detector and then forming the ratio of the output signal of the lock-in to the dc signal. A ratio amplifier was constructed from a Burr-Brown 4096 multiplier following the manufacturer's suggested circuit. The linear polarizer, in a ball-bearing mount, is spun by a synchronous motor at 25 revolutions per second. The reference signal is obtained from a small photodiode which senses a light signal that is chopped by the rotating housing.

To carry out accurate measurements of P, it is necessary to correct carefully for the instrumental polarization of the light-detection system, particularly for small values of P. Many "unpolarized" light sources were tried, and we found that a light bulb spinning on axis at 3600 rpm proved to be the most satisfactory. The calibration was performed as a function of wavelength without altering any part of the optical system. The windows on the reaction chamber ports were independently checked to ascertain that they were free from strain.

III. CHEMILUMINESCENT SPECTRA

We investigated the reactions of Mg, Ca, Sr, and Ba with NO_2 and N_2O. For both oxidizer gases, the light yield was found to increase as we progressed from Mg to Ba. The reaction $Mg + NO_2$ yielded no detectable visible chemiluminescence, and the reaction $Mg + N_2O$ yielded chemiluminescence of such low intensity that little effort was made to pursue the study of this process. The low-resolution spectra of the chemiluminescence from the reactions Ca and Ba with NO_2 and N_2O are presented in Fig. 3. The chemiluminescent spectra of Sr with N_2O is similar to that of $Ba + N_2O$ while that of $Sr + NO_2$ is similar in form to $Ca + NO_2$.

A. General Appearance

An examination of Fig. 3 permits us to classify these spectra into three types. In the case of Ca and Sr with NO_2, the spectra are featureless even at high resolution. In the case of Ca, Sr, and Ba with N_2O, the spectra at low-resolution appear dense and "noisy," but at higher-resolution, these

spectra are shown to be highly structured and comb-like in appearance. Figure 4 illustrates the closely-packed structuring for the case of $Ba + N_2O$. Finally, in the case of $Ba + NO_2$, the spectrum has readily distinguishable band-like features. Indeed, a majority of its bands have been assigned to the A - X blue-green band system of BaO.[10] At higher resolution, as seen in Fig. 5, the rotational structure (partially resolved) is apparent, showing the formation of the bandhead. The shading to the red is characteristic of the BaO A - X system.

Bandheads result from the piling together of a large number of rotational lines.[12] In the case of the BaO A - X system, the bandhead occurs at very low J values ($4 \leq J \leq 6$), so that the bandhead is very close to the band origin;[13] and thus, the width and the rate of degradation (falling off) of the band is a measure of the J' distribution of the v' level. Figure 5 shows four traces of ($v', v'' = 0$) bands that were free from overlap or only weakly overlapped. It is seen that the slope is greatest for ($v' = 6$) and decreases with decreasing v'. Since the exact shape of the band depends on the v' level of the excited state, computer simulations of the shapes of

the four bands were carried out with the same J' distribution for each band, to test the sensitivity of the band profiles to changes of the molecular constants with v'. We found that the shape of the bands (v' = 6, v" = 0) to (v' = 3, v" = 0) were essentially the same for the same J' distribution. Thus we conclude that the band shadings shown in Fig. 5 result from the population of higher J' levels for lower v' levels in the reaction product.

Note that this conclusion is not what would be expected from a phase space argument,[14] but indicates a negative correlation between vibrational and rotational excitation of the BaO product. Similar conclusions have been drawn from the infrared chemiluminescence studies of $F + H_2 \rightarrow HF + H$,[15] and $Cl + H_2 \rightarrow HCl + Cl$,[16] where the rate-of-formation contours in the vibrational-rotational plane show a negative slope.

For reactions with Maxwell-Boltzmann beams, we expect that the rotational distribution of the products will be of a Maxwell-Boltzmann type since a simple model in which (1) the angular momentum of the collision appears as the rotational angular momentum of the products, and (2) the reaction has unit probability for impact parameters less than some critical

value and zero for larger impact parameters, gives this type of distribution. An "effective" rotational temperature may be assigned to the bands shown in Fig. 5, e.g. ($v' = 6$, $v'' = 0$) corresponds approximately to 800° K. Note that the rotational distribution of RbBr products formed in the reaction of the Maxwell-Boltzmann beams $Rb + Br_2$ is also well characterized by a rotational temperature.[4] For the BaO A - X system, the P and R lines alternately blend together and draw apart as a function of increasing J. Consequently, a detailed fit to the band contours is not very informative, particularly since there are underlying contributions from other bands.

B. Pressure Dependence

To determine the mechanism for the light production, it is necessary to know the molecularity of the reaction responsible for the chemiluminescence. This can be studied in LABSTAR by varying the pressure of the gas "beam" and the metal beam while measuring the intensity of the chemiluminescence.

Previously, the Ca + NO_2 chemiluminescence was found

to be second order in the NO_2 pressure, while $Ca + N_2O$, $Ba + N_2O$, and $Ba + NO_2$ were first-order in the oxidizer gas.[10] We measured the pressure dependence of chemiluminescence for the reactions $Sr + NO_2$ and $Sr + N_2O$ (see Fig. 6), and found that the $Sr + NO_2$ chemiluminescence is second order in NO_2, while $Sr + N_2O$ chemiluminescence is first order in N_2O.

A study of the light intensity as a function of metal-atom flux was also carried out. For the $Ba + NO_2$ reaction (in which we have identified the emitter), the intensity may be assumed to depend on the collision of one Ba atom with one NO_2 molecule. Thus, for a fixed gas pressure of NO_2, the chemiluminescence is expected to be proportional to the Ba atom flux. If we vary the Ba atom flux by changing the oven temperature, and measure the chemiluminescence for the reactions with NO_2 and and N_2O both at fixed pressures, then we can determine the metal-atom dependence of the $Ba + N_2O$ reaction. By recalling that the spectra of the reactions of Ba, Sr, and Ca with N_2O all have the same comb-like appearance, we can conclude that these reactions have the same metal-atom

dependence. In Fig. 7a, we present a plot of the $Ba + NO_2$ chemiluminescent intensity versus the $Ba + N_2O$ emission. Figure 7b shows the corresponding plot for Sr. In both cases the data at low pressure are fit satisfactorily by a straight line. We thus conclude that the metal-atom dependence for the reaction with NO_2 is the same as for Ba and Sr. In the case of Ba, we know that the reaction of Ba with NO_2 is first order in both reagents and thus $Ba + N_2O$ is first order in both reagents. By recalling that the spectra of the reactions of Ba and Sr with N_2O both have the same comb-like structure, we can expect that these reactions have the same metal dependence, namely they are first order. Thus we conclude that all four reactions are first order in the metal atom concentration.

Over the range of oven temperatures used, we expect no variation of the total cross section or the (v', J') distribution caused by the change in kinetic energy of the metal beam temperature. The vapor pressure of the alkaline earth metals changes rapidly with small temperature increments. For example, a 10° C increase in the temperature around 1000° C will increase the vapor pressure by 50%.[17]

For such a small change in temperature, the thermal energy of the beam changes inconsequentially (about 0.001 eV out of 0.1 eV or 1%) with respect to the translational energy, which in turn is negligible in comparison to the exothermicity of the reaction.

The spectrometer looks at an area about 4 cm from the hole in the bulkhead through which the metal beam effuses. Since the spectrometer only accepts light from this reaction region, any attenuation of the metal-atom beam by the gas will appear in the pressure dependence of the chemiluminescence. This accounts for the maximum that appears in Fig. 6b. We can derive an expression for the chemiluminescence as a function of gas pressure in terms of the cross section for all processes that remove metal atoms from the beam.[10] By fitting the chemiluminescent intensity I to an expression of the form $P^n \exp(-\alpha P)$, where n is the reaction order in the pressure P of the oxidized gas, we obtain the extinction coefficient α, which is equal to the product of the total cross section σ and the path length ℓ. The total cross sections as well as the molecularity of the reactions are listed in Table I, where it is seen that the cross sections for reaction with

NO_2 are much larger than those with N_2O. The reliability of these cross sections depend on the absolute pressure measurements of the oxidizer gases. The pressure was determined using a Bayard-Alpert ionization gauge located about 20 cm from the center of the reaction chamber (instead of over the diffusion pump as shown in Fig. 1 and as used in Ref. 10). Its sensitivity for NO_2 is assumed to be the same as for N_2O but a factor 1.5 larger than for air.[18] The error in the cross sections given in Table I are almost completely dependent on the error in the absolute pressure measurements which we estimate to be ±50%.

The large difference between the overall reaction rates for these two oxidizer gases can be observed visually.[10] Photographs taken through the observation window in LABSTAR are presented in Fig. 8, showing the chemiluminescence of Ba with NO_2 and N_2O at three different pressures. At low pressures (0.2 millitorr), as shown in Figs. 8a and 8d, the $Ba + N_2O$ and $Ba + NO_2$ reactions have the same visual appearance. At intermediate pressures (0.6 millitorr), Fig. 8b shows that the emission seems to spread out

for the reaction of $Ba + N_2O$; while for $Ba + NO_2$ shown in Fig. 8e the emission, which appears to be confined to the Ba beam, is slightly shortened. At even higher pressures (about 2 millitorr), the difference between $Ba + N_2O$ (Fig. 8c), and $Ba + NO_2$ (Fig. 8f) is even more dramatic. Figure 8 is the pictorial counterpart of Fig. 6, showing the different ratio of nonreactive large-angle scattering to reactive scattering for the two types of reactions.

The light intensity for the group IIA metals with N_2O is greater than with NO_2, although the cross section for beam removal is larger for the NO_2 reactions. The cross sections shown in Table I refer to the sum of the cross sections for all reactive processes that produce electronically excited and ground-state products and the sum of all scattering cross sections that deplete the metal beam. When the cross sections are large, as in the case of the NO_2 chemiluminescence, the cross sections are almost entirely composed of the sum of reactive cross sections for metal-beam removal. The fact that the NO_2 chemiluminescence is weaker than the N_2O chemiluminescence indicates that there is a large cross section for reaction with NO_2 that

does not yield visible emission. We believe the formation of vibrationally excited ground-state metal oxides is predominantly responsible for this large cross section, although we cannot rule out the formation of metal peroxides.

C. Energy Balance

Metal-oxide dissociation energies are notoriously difficult to measure. There are three well-recognized methods for determining $D_0^\circ(MO)$, namely, Birge-Sponer extrapolations, mass spectrometric studies using Knudsen-cell effusion, and flame spectrophotometry, but they yield in general quite disparate results.[19] To help determine the MO dissociation energy, the observation of the short-wavelength limit of the chemiluminescence may be used to place a lower bound on $D_0^\circ(MO)$.

For the reaction

$$M + OQ \rightarrow MO^* + Q \ ,$$

where a metal atom M and an oxidizer gas OQ react to form an electronically excited metal-oxide molecule MO* and a

fragment Q, the exothermicity will depend primarily on the difference between the MO and the OQ bond strengths, denoted by $D_o^\circ(MO)$ and $D_o^\circ(OQ)$, respectively. In the center-of-mass frame, the reactants have a relative translational energy denoted by $E_t(M-OQ)$, and the products have a relative translational energy $E_t(MO^*-Q)$. In addition, the reactants have an internal energy $E_i(OQ)+E_i(M)$. For the oven temperatures used, there is a negligible fraction of metal atoms in excited states, so that $E_i(M)$ is zero. The products have internal excitation energies denoted by $E_i(MO^*)$ and $E_i(Q)$. We thus obtain the energy-balance equation

$$D_o^\circ(MO)+E_i(OQ)+E_t(M-OQ)= D_o^\circ(OQ)+E_i(MO^*)+E_i(Q)+E_t(MO^*-Q)\ , \qquad (2)$$

which may be solved for $D_o^\circ(MO)$ to yield the expression

$$D_o^\circ(MO)=D_o^\circ(OQ)+E_i(MO^*)+[E_i(Q)-E_i(OQ)]+[E_t(MO^*-Q)-E_t(M-OQ)]\ . \qquad (3)$$

We may identify $E_i(MO^*)$ as the short-wavelength limit

of the chemiluminescence, if we assume the emission to be to the ground state. If the emission is to an excited state of the MO molecule, then the short-wavelength limit is an underestimate of $E_i(MO^*)$. The internal energy of the oxidizer gas corresponds to the thermal energy of OQ, and is expected to be less than or equal to the internal excitation energy of the freshly-formed fragment Q. As will be explained in III D, the translational energies of the reactants and products are likely to be comparable for reactions with NO_2. For reactions with N_2O, we may assume $E_t(MO^* - Q)$ to be somewhat greater than $E_t(M - OQ)$. We obtain the inequality

$$D_0^\circ(MO) \geq D_0^\circ(OQ) + E_i(MO^*) - [E_i(OQ) + E_t(M - OQ)] \quad . \qquad (4)$$

For thermal beams we estimate $E_i(OQ) + E_t(M - OQ)$ to be 0.1 eV. The energy required to rupture the NO - O bond in NO_2 is 3.115 eV,[20] and the short-wavelength limit was determined to correspond to 2.68 eV. Thus from the reaction of $Ba + NO_2$ to yield $BaO^* + NO$, we find $D_0^\circ(BaO) \geq 5.70$ eV (131.5 kcal/mole). This compares favorably with the dissociation energies recommended by Gaydon[19] (133 ±3 kcal/mole) and by Brewer and Rosenblatt[21] (131 ±6 kcal/mole). This agreement lends support

to our supposition that the relations $E_t(MO^* - Q) \simeq E_t(M - OQ)$ and $E_i(Q) \simeq E_i(OQ)$ hold. Note that by obtaining a strict lower bound to the BaO dissociation energy one can eliminate from consideration many of the previous determinations by other methods.[19,21]

If we attempt to treat the reaction $Ba + N_2O \rightarrow BaO^* + N_2$ in a similar manner, the short-wavelength cutoff implies that $D_0^\circ(BaO) \geq 5.2$ eV. Based on our lower bound for the reaction $Ba + NO_2$, an amount of energy totalling 0.5 eV is unaccounted for. We conclude that either the BaO electronic transition does not terminate on the ground state (but rather on a state about 0.5 eV above the ground state), or the N_2 fragment has high internal excitation.

D. Mechanisms for NO_2 Reactions

The magnitude of the cross sections (see Table I) for the reactions of the alkaline earth metals with NO_2 is 50 to 100 times gas kinetic and is reminiscent of the alkali-atom-halogen-molecule reactions. The latter have been successfully explained in terms of the electron-jump model (harpoon

mechanism), whereby an electron is transferred from the alkali atom to the halogen molecule as the two approach one another. The electrostatic attraction between the ion pair "reels in" the halogen atom to form the salt molecule while the other halogen atom plays the role of a spectator (spectator-stripping model).[21] The electron-jump model can also explain quite satisfactorily the large cross sections for any of the reactions of the group IIA metals with NO_2.

According to the electron-jump model, the distance r_c (at which the electron transfers) corresponds to the curve crossing of the ionic and covalent potentials:

$$e^2/r_c = IP(M) - E_v(OQ) \quad , \tag{5}$$

where IP(M) is the ionization potential of the metal atom and $E_v(OQ)$ the vertical electron affinity of the oxidizer gas OQ. The reactive cross section is then estimated to be simply πr_c^2.

For the reactions of NO_2 with Ca, Sr, and Ba, Table I lists the cross sections calculated from the electron-jump model where we have used the well-known ionization

potentials of the alkaline earth metals[23] and the value of 3.15 eV for the NO_2 vertical electron affinity.[20,25] The electron-jump model yields not only the correct ordering of the cross sections (which is not too surprising), but also the approximate ratios of the cross sections. Note that the electron affinity of NO_2 (3.15 eV) is quite comparable to the energy required to rupture the NO - O bond (3.115 eV), which suggests that the O atom readily separates from NO_2 after electron transfer. The bond length of the N - O bond in NO_2 is 1.19 Å,[20] while in NO it is 1.15 Å.[12] Thus the NO fragment is not expected to be appreciably excited, and its translational energy in this model would be very similar to the initial translational energy of the NO_2 molecule (see Section III C). The electron-jump model also predicts that the angular distribution of the BaO product would be peaked in the forward direction (analogous to the reactions of $K + Br_2$).

We wish to emphasize again that the measured cross sections in Table I refer to the cross sections for beam attenuation and are not necessarily the cross sections for producing a light-emitting species. Indeed, the comparison

between the chemiluminescence intensities for NO_2 and N_2O shows that the cross sections for NO_2 reactions in Table I refer almost entirely to "invisible reactions", namely to the formation of what we believe to be the vibrationally-excited ground-state metal oxide. For the reactions of Ca and Sr with NO_2, which are second order in NO_2, we believe that a subsequent collision of the vibrationally excited metal-oxide molecule with NO_2 forms some polyatomic species responsible for the chemiluminescence. This mechanism is consistent with the broad featureless emission spectrum from these reactions, the weakness in emission intensity, and the large measured cross section. The tabulated bond energies for CaO and SrO are uncertain, but if we use Gaydon's recommended values, there is insufficient energy for $Ca + NO_2$ or $Sr + NO_2$ to yield CaO or SrO in an electronically excited state (at least, one that emits in the visible).[19] Moreover, this rules out the possibility that the chemiluminescence is caused by the vibrational-electronic transfer $MO^{\dagger} + NO_2 \rightarrow MO + NO_2^{*}$, whereby an electronically excited NO_2 molecule is generated and the vibrationally excited MO molecule is quenched.

E. Mechanisms for N_2O Reactions

In contrast to those for NO_2, the cross sections for the reactions of the alkaline earth metals with N_2O are much smaller even though the N_2O reactions are more exothermic. The electron-jump model does not apply to the reaction with N_2O, since the N_2O molecule has a very small or even negative vertical electron affinity, even though the N_2O negative ion is known to exist from mass spectrometric work.[26] The small vertical electron affinity arises from the fact that the ground state of N_2O negative ion is linear; while the ground state of N_2O^-, which is isoelectronic to NO_2, is believed to be bent.[27]

It seems reasonable to assume then that the reactions of the group IIA metals with N_2O result primarily from close-in encounters. The ground state of the N_2O molecule is a $^1\Sigma^+$ state and does not correlate with the ground-state fragments, but with $N_2(^1\Sigma_g^+) + O(^1D)$. Thus there is a curve-crossing between the $N_2(^1\Sigma_g^+) + O(^3P)$ and $N_2(^1\Sigma_g^+) + O(^1D)$ potential curves.[28] We suggest that the interaction of M with N_2O in the vicinity of the singlet-triplet crossover causes the MO

product to be formed in an excited triplet state. This spin-nonconserving mechanism is consistent with the small cross section we have found; it can help to explain the comb-like appearance of the N_2O chemiluminescent spectrum because of the more complex bandhead appearance of the triplet-triplet transitions (see Fig. 4), and it accounts for the 0.5 eV excess energy previously mentioned in III C.

In the CaO and SrO molecules the relative ordering of the triplet and singlet electronic states is not known and the nature of the ground state is still open to question. However in the BaO molecule, molecular beam electric and magnetic resonance studies indicate that the ground state is a $^1\Sigma$ state.[29,30] Moreover, it has been estimated from the magnitude of the rotational magnetic moment that no triplet states lie less than 10,000 cm^{-1} above the BaO ground state. This estimate is in conflict with our interpretation of the $Ba + N_2O$ chemiluminescence as being caused by a triplet-triplet electronic transition whose lowest state terminates about 4,000 cm^{-1} above the ground state. Indeed, no triplet-triplet band system in BaO has ever been definitely identified, although the BaO

$A\,^1\Sigma - X\,^1\Sigma$ band system shows a large number of perturbations which may owe their origin to triplet states.[13,31] Intensity considerations and the highly-structured nature of the spectrum would appear to rule out two-body radiative association as a possible mechanism for the $Ba + N_2O$ chemiluminescence.

IV. CHEMILUMINESCENT POLARIZATION

Using the spinning polarizer set-up shown schematically in Fig. 2, we measured the degree of polarization of the chemiluminescence from the reaction of some of the group IIA metals with NO_2 and N_2O. The emission from several different vibrational bands of BaO* formed from $Ba + NO_2$ was found to be weakly polarized (see Table II), and the apparent trend with v' excitation awaits further study. The reaction of $Ba + N_2O$ and $Sr + N_2O$ also produced weakly polarized chemiluminescence ($P \leq 5\%$). However, for the reaction of $Sr + NO_2$, in which the light production is quadratic in the NO_2 concentration, no polarization was detectable.

The appearance of the polarized emission implies that the products "remember" that they are formed from an anisotropic relative velocity distribution of the reactants. An oversimplified model of the chemical reaction serves to show how conservation of total angular momentum endows the products with this "memory" of their mode of formation. Let A and B combine to form AB*, where B is stationary, and A travel along the Z direction. Then the total angular momentum vector

of AB* lies in a plane perpendicular to Z. The anisotropic distribution of the AB* angular momentum causes the fluorescence from AB* to be polarized.

For a more realistic model, let $\underset{\sim}{L}_i$ and $\underset{\sim}{L}_f$ denote the initial and final orbital angular momentum vectors of the collision partners, and let $\underset{\sim}{J}_X$ represent the internal angular momentum vector of the species X. Then for the reaction $A + BC \rightarrow AB^* + C$ we may write[32]

$$\underset{\sim}{L}_i + \underset{\sim}{J}_i = \underset{\sim}{L}_f + \underset{\sim}{J}_f \ , \tag{6}$$

where

$$\underset{\sim}{J}_i = \underset{\sim}{J}_A + \underset{\sim}{J}_{BC} \ , \tag{7}$$

and

$$\underset{\sim}{J}_f = \underset{\sim}{J}_{AB^*} + \underset{\sim}{J}_C \ . \tag{8}$$

The initial internal angular momentum vectors $\underset{\sim}{J}_A$ and $\underset{\sim}{J}_{BC}$ are randomly oriented, whereas the initial orbital angular momentum vector $\underset{\sim}{L}_i$ lies in a plane at right angles to the initial relative velocity vector $\underset{\sim}{v}$. Consequently, the total angular momentum of the system always has a cylindrical distribution

about $\underset{\sim}{v}$.

The magnitude of $\underset{\sim}{L}_i$ may be estimated classically as the product of the reduced mass μ of the reactants, their initial relative velocity v, and their impact parameter b. For large reactive cross sections corresponding to the reaction at large impact parameters, $|\underset{\sim}{L}_i|$ is on the order of several hundred $\hbar$. The magnitude of $\underset{\sim}{J}_i$ depends primarily on the rotational angular momentum of the molecule when A is an atom. For moderate temperatures and moderate moments of inertia $|\underset{\sim}{J}_i|$ is on the order of 10 to 30 $\hbar$. Thus for most chemical reactions with large cross sections, we find $|\underset{\sim}{L}_i| >> |\underset{\sim}{J}_i|$. We consider the limiting case where $|\underset{\sim}{J}_i|$ may be ignored when compared to $|\underset{\sim}{L}_i|$. Then the total angular momentum of the reactants and hence the products must lie in a plane perpendicular to $\underset{\sim}{v}$. The correlation of the internal angular momentum distribution of the products with the direction of $\underset{\sim}{v}$ will then depend in detail on how the total angular momentum is partitioned in magnitude and direction into $\underset{\sim}{L}_f$ and $\underset{\sim}{J}_f$.

Let us further assume[33] $|\underset{\sim}{J}_f| >> |\underset{\sim}{L}_f|$; i.e. most of the angular momentum appears as rotational rather than recoil

angular momentum of the products. Then $\underset{\sim}{J}_f$ will lie almost parallel to $\underset{\sim}{L}_i$, and the products will be formed with an anisotropic angular momentum distribution which will manifest itself through the polarization of the AB* fluorescence. For large rotational angular momenta, the radiative process of the AB* molecule may be treated classically where the transition dipole moment for emission of light will be either along $\underset{\sim}{J} = \underset{\sim}{J}_{AB^*}$ or will lie in a plane perpendicular to the molecular axis, and the transition is traditionally referred to as a perpendicular-type ($\perp$); in the latter case, the transition moment lies along the internuclear axis, and the transition is traditionally referred to as a parallel-type ($\parallel$). Given the type of transition and the distribution of $\underset{\sim}{J}$ vectors of the molecule, we can calculate the degree of polarization of the light emitted into an arbitrary direction.

Let $\hat{n}$ be a unit vector perpendicular to the direction of observation, and let $\hat{J}$ be a unit vector along $\underset{\sim}{J}$ with the distribution $f(\theta,\varphi)$. For a penpendicular-type transition, the intensity of light polarized along $\hat{n}$ is proportional to

$$I_n^{\perp} = \int_0^{2\pi} \int_0^{\pi} (\hat{n} \cdot \hat{J})^2 \; f(\theta,\varphi) \; \sin\theta d\theta d\varphi \; . \qquad (9)$$

From Eq. (9) it follows that the intensity polarized along the Z axis is proportional to

$$I_Z^{\perp} = \int_0^{2\pi} \int_0^{\pi} \cos^2\theta \; f(\theta,\varphi) \; \sin\theta d\theta d\varphi \; , \qquad (10)$$

while the intensity polarized along the X axis is proportional to

$$I_X^{\perp} = \int_0^{2\pi} \int_0^{\pi} \sin^2\theta \cos^2\varphi \; f(\theta,\varphi) \; \sin\theta d\theta d\varphi \; . \qquad (11)$$

Similarly, for a parallel-type transition, one can show[34]

$$I_n^{\parallel} = \tfrac{1}{2} \int^{2\pi} \int^{\pi} [1 - (\hat{n} \cdot \hat{J})^2] \; f(\theta,\varphi) \; \sin\theta d\theta d\varphi \; , \qquad (12)$$

so that $I_n^{\perp} + 2I_n^{\parallel}$ is independent of the direction of $\hat{n}$. It then follows that

$$I_Z^{\parallel} = \tfrac{1}{2} \int_0^{2\pi} \int_0^{\pi} \sin^2\theta \; f(\theta,\varphi) \; \sin\theta d\theta d\varphi \; , \qquad (13)$$

and

$$I_X^{\parallel} = \tfrac{1}{2} \int_0^{2\pi} \int_0^{\pi} (1 - \sin^2\theta \cos^2\varphi) \; f(\theta,\varphi) \; \sin\theta d\theta d\varphi \; . \qquad (14)$$

As a consequence of the spherical harmonic addition

theorem, we derive

$$[\hat{n}(\theta_o,\varphi_o)\cdot\hat{J}(\theta,\varphi)]^2 = \tfrac{1}{5}\Big[(8\pi/5)\sum_{m=-2}^{2} Y_{2m}(\theta_o,\varphi_o)\,Y^*_{2m}(\theta,\varphi) + 1\Big] \ . \quad (15)$$

A substitution of this result into Eqs. (9) and (12) shows that the angular distribution of light emitted in an electric dipole transition is a linear combination of spherical harmonics, of order two and zero, which can be characterized by six parameters (5 coefficients for the Y_{2m} terms and 1 coefficient for the constant term). Thus we find that the dipole-radiation pattern blurs an arbitrarily sharp $f(\theta,\varphi)$ distribution, so that the angular distribution $I(\theta,\varphi)$ of the light intensity is in general much smoother than the $f(\theta,\varphi)$ distribution of the angular momentum vectors.

In our experimental study of $Ba + NO_2$ to yield BaO* chemiluminescence, the beam of Ba atoms may be regarded as impinging on a scattering cell filled with NO_2 gas. Thus $f(\theta,\varphi)$ is expected to have cylindrical symmetry about the metal-beam direction which defines the Z axis.[35] We may write

$$f(\theta,\varphi) = \sum_{\ell} a_\ell \, P_\ell(\cos\theta) \ , \quad (16)$$

and it follows that the degree of polarization P is given by

$$P(\perp\text{-type transition}) = 3a_2/(10a_0 + a_2) \ , \qquad (17)$$

and

$$P(\parallel\text{-type transition}) = -3a_2/(20a_0 - a_2) \ . \qquad (18)$$

From Eqs. (17) and (18) it is apparent for cylindrical symmetry in $f(\theta,\varphi)$, that a measurement of the degree of polarization at a fixed observation direction gives the <u>same</u> information as a measurement of the angular distribution of the light intensity.

In the case we have just discussed of a beam reacting with a gas and in the case of two well-collimated and velocity-selected crossed beams, both have cylindrical symmetry, the former about the beam, the latter about the relative velocity vector. However, for two Maxwell-Boltzmann crossed beams, there is only a plane of symmetry defined by the two beam directions, so that the absolute magnitude of the coefficient of Y_{2m} is the same as $Y_{2,-m}$.[36]

In the reaction $Ba + NO_2$, the degree of polarization may be estimated by assuming that all initial orbital angular

momentum of the reactive collision appears as rotational angular momentum of the BaO* product; i.e. $\underset{\sim}{L}_i = \underset{\sim}{J}_{BaO^*}$. This limiting model would then be expected to provide an upper bound to P. The calculational procedure is to (1) find the distribution of relative velocity vectors,

$$\underset{\sim}{v}_{rel} = \underset{\sim}{v}_{Ba} - \underset{\sim}{v}_{NO_2} , \tag{19}$$

using the method of Markoff,[30] (2) determine the angular distribution of $\underset{\sim}{J}$ vectors for each value of $\underset{\sim}{v}_{rel}$, and (3) calculate the degree of polarization for this parallel-type transition (BaO $A^1\Sigma - X^1\Sigma$) using Eq. (18). The calculations are reasonably involved but straightforward.

Let the beam velocity $\underset{\sim}{v}_b$ be along the positive Z axis, and let the velocity of the NO_2 gas have a distribution $\exp(-m\underset{\sim}{v}^2/2kT)$, where $\underset{\sim}{v}$ is the velocity and m is the mass of the NO_2 scattering gas. Then we can write for the distribution of the relative velocity vectors

$$P(\underset{\sim}{v}_{rel}) = \int d^3v \exp(-mv^2/2kT)\ \delta^3(\underset{\sim}{v}_{rel} - \underset{\sim}{v}_b + \underset{\sim}{v}) . \tag{20}$$

The δ-function may be replaced by its integral representation

$$\delta^3(\underset{\sim}{q}) = \int \exp(-i\underset{\sim}{\rho}\cdot\underset{\sim}{q})\,d^3\rho \ . \tag{21}$$

Hence,

$$P(\underset{\sim}{v}_{rel}) = \exp[-m(v_{rel}^2 + v_b^2 - 2v_{rel}\,v_b\cos\gamma)/2kT] \ , \tag{22}$$

where γ is the angle between $\underset{\sim}{v}_{rel}$ and the Z axis.

To find the probability that the product is formed with its rotational angular momentum vector $\underset{\sim}{J}$ making an angle θ with respect to the Z axis, we must integrate over all relative velocity vectors lying in a plane perpendicular to $\underset{\sim}{J}$. For a given $\underset{\sim}{J}$ we have

$$J(\theta) = \exp[-m(v_{rel}^2 + v_b^2)/2kT]\int_0^{2\pi} \exp(m\,v_{rel}\,v_b\sin\theta\cos\beta/kT)\,d\beta \ , \tag{23}$$

where β is the azimuthal angle about $\underset{\sim}{J}$. Using the integral representation[38] for the Bessel function

$$J_0(z) = \pi^{-1}\int_0^{\pi} \exp(i\,z\cos\beta)\,d\beta \tag{24}$$

and the fact

$$J_0(-z) = J_0(z) \ , \tag{25}$$

we may reduce Eq. (23) to the form

$$J(\theta) = \exp[-m(v_{rel}^2 + v_b^2)/2kT]\, J_o(i\, m\, v_{rel}\, v_b \sin\theta/kT) \quad . \qquad (26)$$

Equation (26) represents the angular distribution of the $\underset{\sim}{J}$ vector which may be written as

$$J(\theta) = f(\theta, v_{rel}, v_b)$$

$$= \sum_{\ell} a_{\ell}(v_{rel}, v_b)\, P_{\ell}(\cos\theta) \quad . \qquad (27)$$

Using Sonine's first integral[38]

$$J_{\mu+\nu+1}(z) = z^{\nu+1}[2^{\nu}\Gamma(\nu+1)]^{-1}$$

$$\times \int_o^{\pi/2} J_{\mu}(z \sin\theta) \sin^{\mu+1}\theta \cos^{2\nu+1}\theta d\theta \quad , \qquad (28)$$

which is valid provided that the real part of μ and ν exceed -1, we find

$$a_0 = \tfrac{1}{2} \exp[-m(v_{rel}^2 + v_b^2)/2kT] \sinh X/X \quad , \qquad (29)$$

and

$$a_2 = \tfrac{5}{4} \exp[-m(v_{rel}^2 + v_b^2)/2kT]$$

$$\times [3X^{-1} \cosh X/X - (3X^{-2} + 1) \sinh X/X] \quad , \qquad (30)$$

where

$$X = m v_{rel} v_b / 2kT \ . \qquad (31)$$

Figure 9 shows P as a function of the dimensionless parameter X for a parallel-type transition. At very small values of X, P approaches zero; while at large values of X, P approaches 1/3. It is not easy to estimate an appropriate average value of $\bar{X}$ for our experimental conditions, although we believe $\bar{X}$ will be in the range 0.5 to 2.0, corresponding to P = 0.006 to P = 0.071. Our experimental measurements of P given in Table II correspond to $\bar{X} = 1$. A more detailed analysis of the model would require us to perform the necessary averages over the distributions in $\underset{\sim}{v}_b$ and $\underset{\sim}{v}_{rel}$ as well as to take into account the dependence of the cross section on relative velocity. However, we do not believe it is worthwhile to pursue this matter further because of the simplicity of the model. Nevertheless we can conclude that a fair fraction of the total angular momentum of the reactive collision in the case of $Ba + NO_2$ appears as rotational excitation of the BaO* product.

In summary, polarization measurements have the potential of providing information about the partitioning of the total angular momentum into rotational and recoil

angular momenta of the products. Moreover, polarization measurements can be carried out in principle as a function of the vibrational and rotational excitation of the newly formed products.

TABLE I. Chemiluminescent Reaction Kinetics.

Reaction	Order of Reaction[a]	Measured Cross Section ($Å^2$)	Calculated Cross Section ($Å^2$)[b]
$Ba + N_2O$	First	27	
$Ba + NO_2$	First	165	150
$Sr + N_2O$	First	$\leq$ 27	
$Sr + NO_2$	Second	127	100
$Ca + N_2O$	First	16	
$Ca + NO_2$	Second	93	70

[a] The order of the reaction is the order in gas pressure. All reactions appear to be first order in metal.

[b] Cross sections are calculated using an electron-jump model.

TABLE II. Polarization of Ba + NO_2 Chemiluminescence. The assignment of the (v', v") band to the observed polarization is somewhat ambiguous because of overlapping bands at the resolution used (10-Å spectral slitwidth).

Wavelength (Å)	Band	Degree of Polarization
4983	(7,0)	2.5 %
5140	(6,0)	2.2 %
5210	(5,0)	1.9 %
5340	(4,0)	1.4 %
5520	(3,0)	1.2 %

REFERENCES

1. See, for example, T. H. Bull and P. B. Moon, Disc. Farad. Soc. 17, 54 (1954); E. H. Taylor and S. Datz, J. Chem. Phys. 23, 1711 (1955); E. F. Greene, R. W. Roberts, and J. Ross, J. Chem. Phys. 32, 940 (1960); D. R. Herschbach, G. H. Kwei, and J. A. Norris, J. Chem. Phys. 34, 1842 (1961).

2. For recent reviews consult D. R. Herschbach, Advan. Chem. Phys. 10, 319 (1966); M. J. Henchman, Ann. Rept. Chem. Soc. (London) 62, 39 (1966); A. R. Blythe, M. A. D. Fluendy, and K. P. Lawley, Quart. Rev. (London) 20, 465 (1966); E. F. Greene and J. Ross, Science 159, 587 (1968); J. P. Toennies, Ber. Bunsenges Physik. Chem. 72, 927 (1968).

3. R. R. Herm and D. R. Herschbach, J. Chem. Phys. 43, 2139 (1965). See also C. Maltz, Ph.D. thesis, Harvard University, 1969.

4. R. Grice, J. E. Mosch, S. A. Safron, and J. P. Toennies, J. Chem. Phys. 53, 3376 (1970).

5. S. M. Freund, G. A. Fisk, D. R. Herschbach, and W. Klemperer, J. Chem. Phys. 54, 2510 (1971).

6. T. P. Schafer, P. E. Siska, J. M. Parson, F. P. Rully, Y. C. Wong, and Y. T. Lee, J. Chem. Phys. 53, 3385 (1970).

7. See K. G. Anlauf, P. E. Charters, D. S. Horne, R. G. Macdonald, D. H. Maylotte, J. C. Polanyi, W. J. Skrlac, D. C. Tardy, and K. B. Woodall, J. Chem. Phys. 53, 4091 (1970) and references cited therein.

8. H. Harrison and D. M. Scattergood, Bull. Am. Phys. Soc. II 10, 1211 (1965); Boeing Technical Document D1-82-0480 (Boeing Scientific Research Laboratories, Seattle, Washington, 1966).

9. M. Ackerman, Bulletin de l'Académie Royale de Belgique 53, 1311 (1967). A. E. Redpath and M. Menzinger (private communication) are presently studying the $NO + O_3$ chemiluminescence under beam conditions as a function of the collision energy.

10. Ch. Ottinger and R. N. Zare, Chem. Phys. Letters 5, 243 (1970).

11. C. D. Jonah and R. N. Zare, Chem. Phys. Letters 9, 65 (1971).

12. G. Herzberg, Spectra of Diatomic Molecules (D. Van Nostrand Co., Inc.; Princeton, New Jersey, 1950).

13. A. Lagerqvist, E. Lind, and R. F. Barrow, Proc. Phys. Soc. Londong 63A, 1132 (1950).

14. P. Pechukas and J. C. Light, J. Chem. Phys. 42,

3281 (1965); P. Pechukas, J. C. Light, and C. Rankin, J. Chem. Phys. 44, 794 (1966).

15. J. C. Polanyi and D. C. Tardy, J. Chem. Phys. 51, 5717 (1969).

16. K. G. Anlauf, J. P. Kuntz, D. H. Maylotte, P. D. Pacey, and J. C. Polanyi, Disc. Farad. Soc. 44, 183 (1967).

17. N. Nesmeyanov, Vapor Pressure of the Elements (Academic Press, New York, 1963), p. 187.

18. S. Dushman and J. M. Lafferty, Scientific Foundations of Vacuum Technique, 2nd Ed. (John Wiley and Sons, Inc., New York, 1962), pp. 301-350, esp. p. 326.

19. A. G. Gaydon, Dissociation Energies, 3rd Ed. (Chapman and Hall, London, 1968).

20. G. Herzberg, Electronic Spectra of Polyatomic Molecules (D. Van Nostrand, Princeton, New Jersey, 1966).

21. L. Brewer and G. M. Rosenblatt, "Dissociation Energies and Free Energy Functions of Gaseous Monoxides" Advances in High Temperature Chemistry, L. Eyring, ed. (Academic Press, Inc., New York, 1969) pp. 1-74.

22. D. R. Herschbach, Advan. Chem. Phys. 10, 319 (1966).

23. C. E. Moore, Ionization Potentials and Ionization Limits Derived from the Analyses of Optical Spectra [Nat. Std. Ref. Data Sur., Nat. Bur. Stand. (U.S.), 34, September 1970].

24. P. Warneck, Chem. Phys. Letters 3, 532 (1969).

25. O. E. Wagner, Bull. Am. Phys. Soc. II 13, 1395 (1968).

26. J. L. Paulson, Advan. Chem. Ser. 58, 28 (1966).

27. E. E. Ferguson, F. C. Fehsenfeld, and A. L. Schmeltekopf, J. Chem. Phys. 47, 3085 (1967).

28. This fact may be responsible for the large quenching cross section observed for $O(^1D)$ colliding with N_2 gas. See M. Lowenstein, J. Chem. Phys. 54, 2282 (1971), and J. F. Noxon, J. Chem. Phys. 52, 1852 (1970).

29. L. Wharton, M. Kaufman, and W. Klemperer, J. Chem. Phys. 37, 621 (1962).

30. R. Brooks and M. Kaufman, J. Chem. Phys. 43, 3406 (1965).

31. I. Kovács and A. Lagerqvist, Arkiv för Fysik 2, 411 (1950).

32. D. R. Herschbach, Disc. Farad. Soc. 33, 149 (1962).

33. D. G. Truhlar, J. Chem. Phys. 54, 2635 (1971) [see also their Refs. (4) and (13)].

34. P. P. Feofilov, The Physical Basis of Polarized Emission (Consultants Bureau Enterprises, Inc., New York, 1961), pp. 277 f.

35. For cylindrical symmetry about the metal-beam direction the term |P| should be a maximum along the beam. This was experimentally verified. By focusing the spectrometer slit at the tip of the gas-inlet orifice, we found the maximum value of P to be tilted from the metal beam direction, as would be expected for crossed beams.

36. This assumes the symmetry plane is the XZ or YZ plane. Polarization measurements along two nonequivalent directions of observation are necessary to determine the four coefficients.

37. S. Chandrasekhar, Rev. Mod. Phys. 15, 2 (1943).

38. G. N. Watson, Theory of Bessel Functions (Cambridge University Press, Cambridge, 1958), pp. 25 and 373.

FIGURE CAPTIONS

Fig. 1. Schematic diagram of LABSTAR.

Fig. 2. Block diagram of apparatus used to measure the degree of polarization.

Fig. 3. Chemiluminescent spectra. These spectra were taken with the 1/3 m Heathkit spectrometer.[10]

Fig. 4. Chemiluminescent spectrum of $Ba + N_2O$ at 0.5 Å spectral slitwidth showing its highly structure nature.

Fig. 5. Four (v', v") bands from the chemiluminescent spectrum of $Ba + NO_2$ which show how the shading changes with v'. In the (3,0) band the 5535-Å Ba line is present.

Fig. 6. Dependence of chemiluminescence on oxidizer gas pressure.

Fig. 7. Chemiluminescence of $M + NO_2$ plotted versus the chemiluminescence of $M + N_2O$ for various metal beam fluxes.

Fig. 8. Photographs of $Ba + N_2O$ chemiluminescence, (a), (b), and (c), and $Ba + NO_2$ chemiluminescence, (d), (e), and (f). The oxidizer gas pressures for (a) and (d) were 0.2 mtorr, for (b) and (e) were 0.6 mtorr, and for (c) and

(f) were 2 mtorr. The photographs were taken at f/2.8 with exposure times of 4-15 sec using high-speed Ektachrome film.

Fig. 9. Polarization calculated for a parallel-type transition as a function of the parameter X.

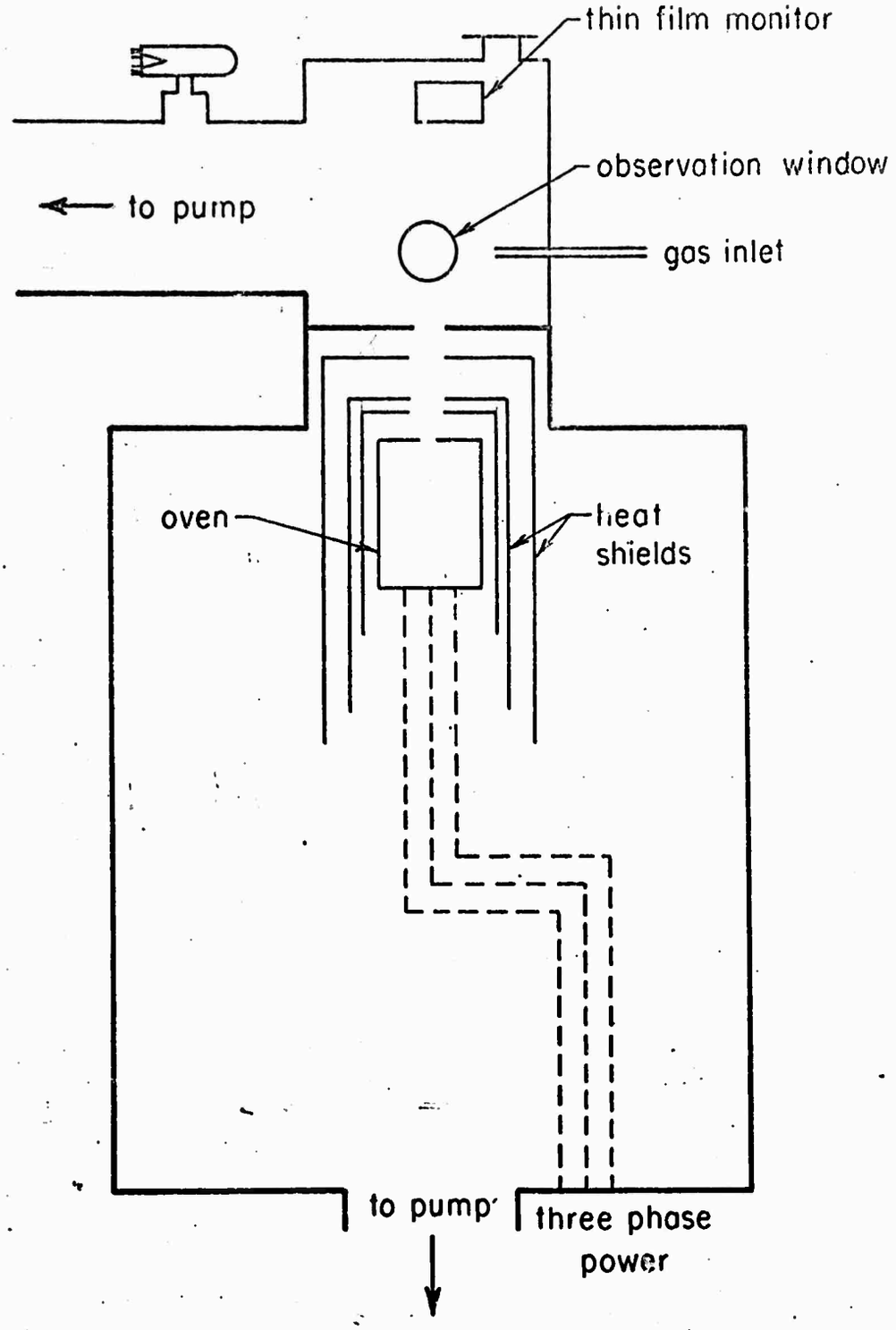
thin film monitor
observation window
to pump
gas inlet
oven
heat
shields
to pump
three phase
power

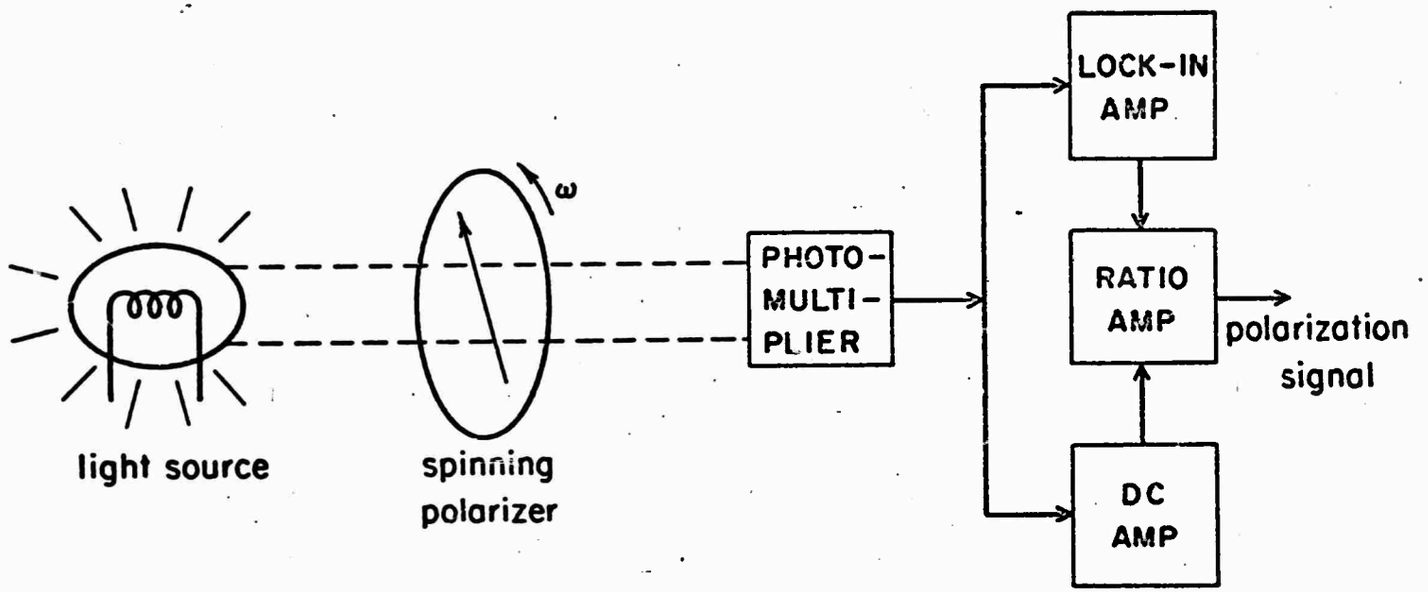
LOCK-IN AMP
RATIO AMP
DC AMP
PHOTO-MULTI-PLIER
ω
polarization signal
light source
spinning polarizer

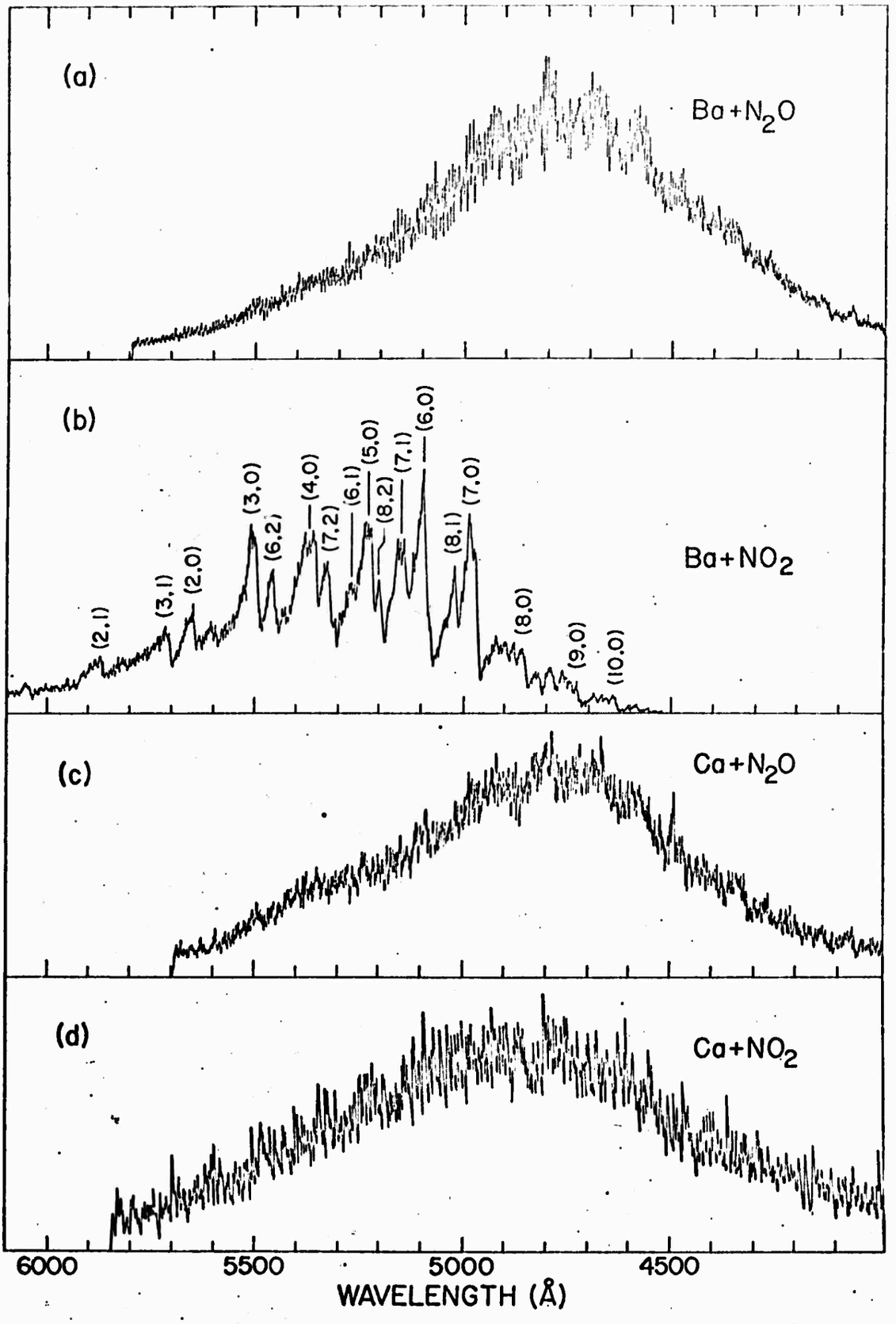
(a)
Ba+N2O
(b)
(2,1)
(3,1)
(2,0)
(3,0)
(6,2)
(4,0)
(7,2)
(6,1)
(5,0)
(8,2)
(7,1)
(6,0)
(8,1)
(7,0)
(8,0)
(9,0)
(10,0)
Ba+NO2
(c)
Ca+N2O
(d)
Ca+NO2
6000
5500
5000
4500
WAVELENGTH (Å)

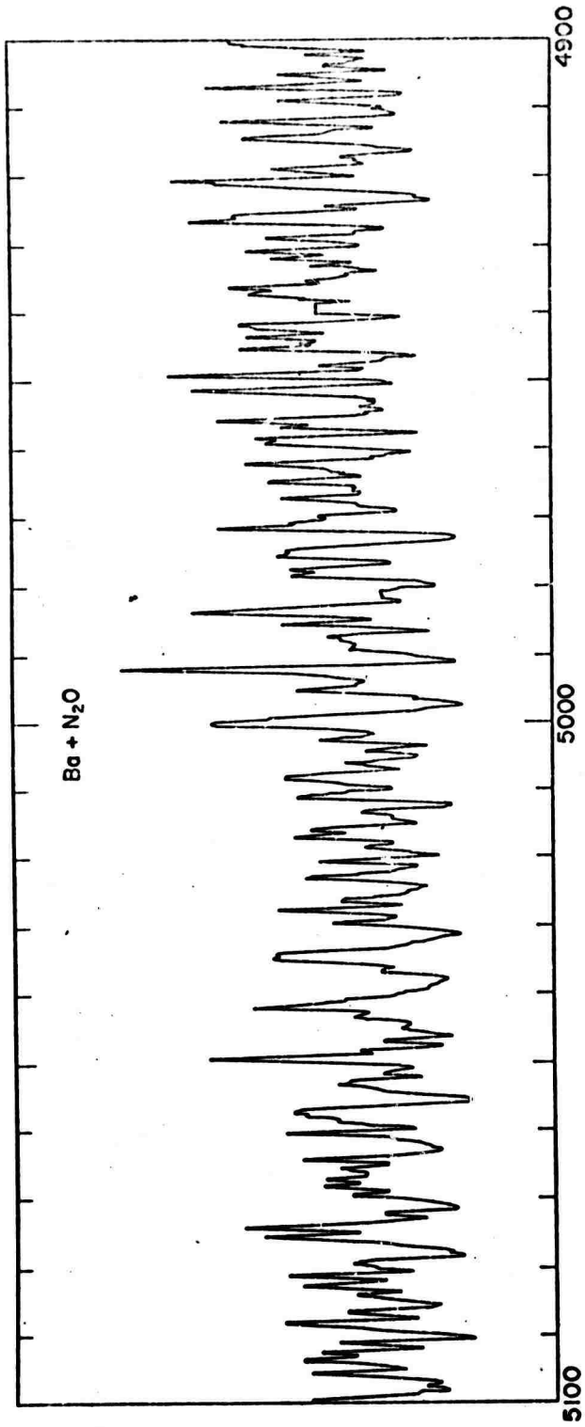
Ba + N2O
4900
5000
5100

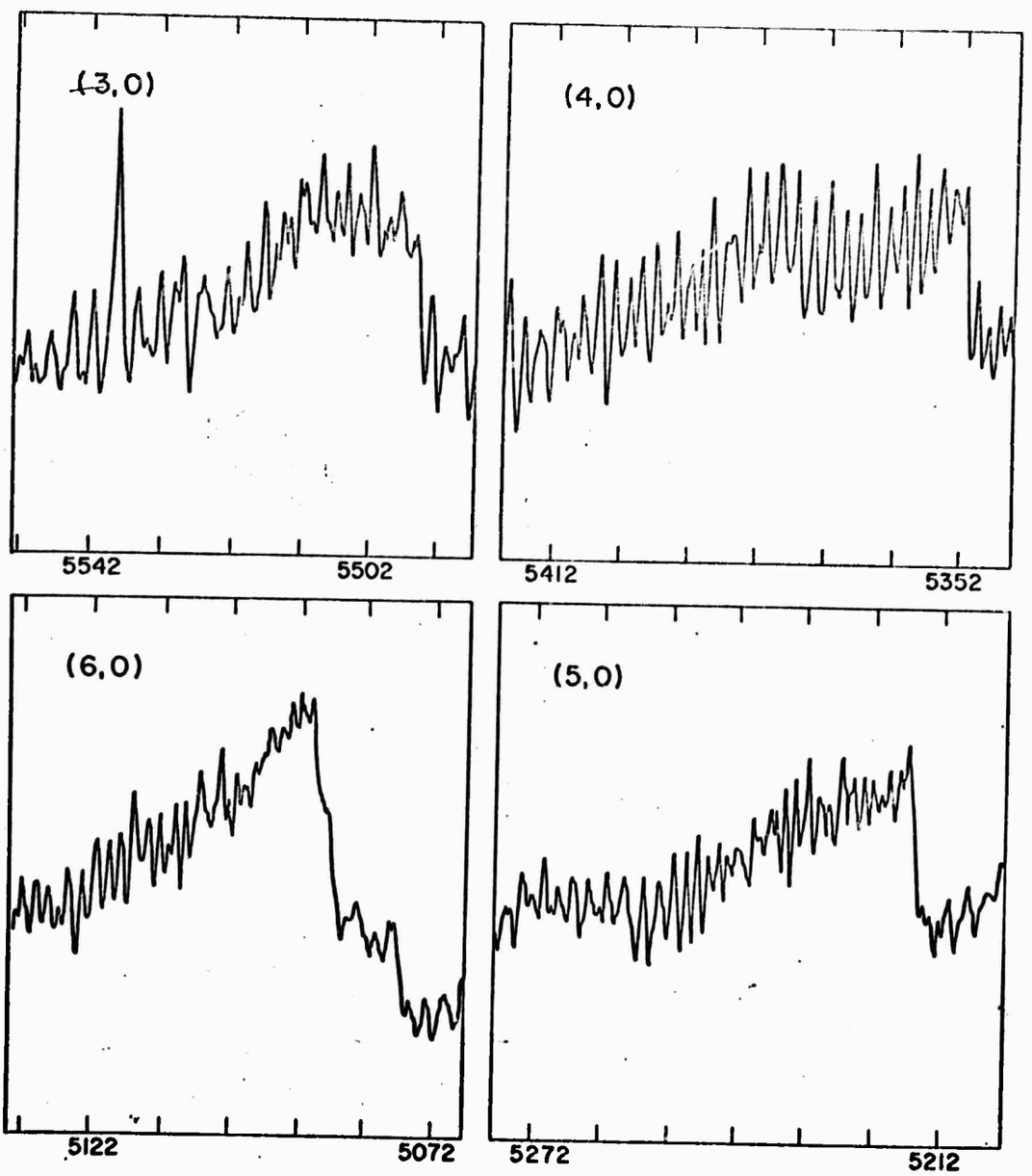
(3,0)
5542
5502
(4,0)
5412
5352
(6,0)
5122
5072
(5,0)
5272
5212

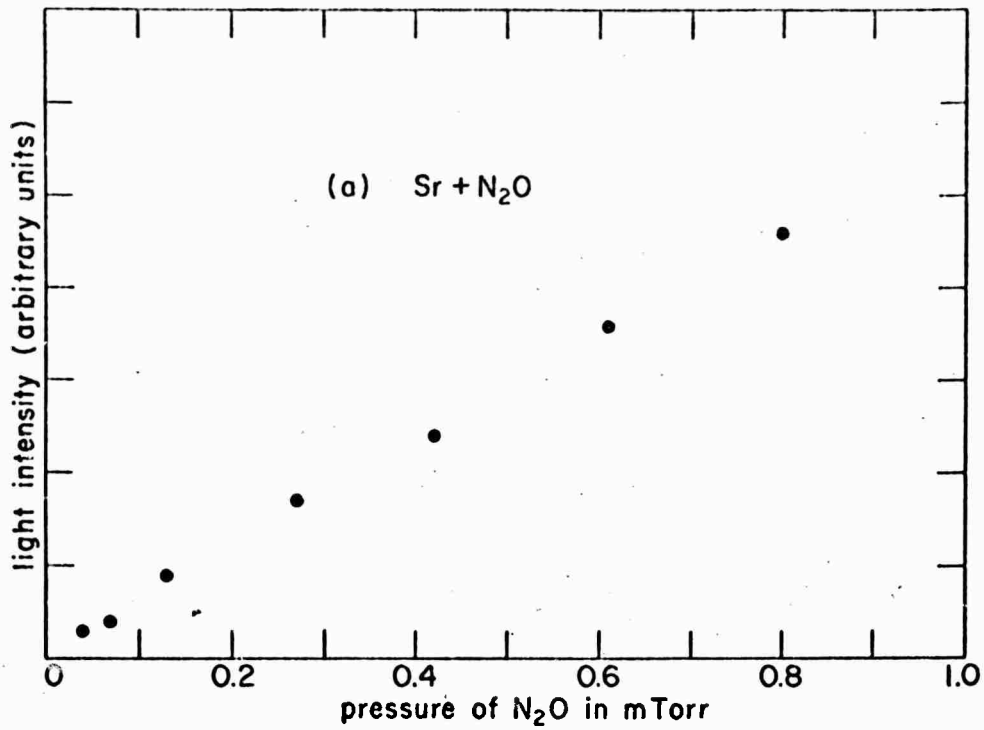
(a) Sr + N_2O
light intensity (arbitrary units)
0
0.2
0.4
0.6
0.8
1.0
pressure of N_2O in mTorr

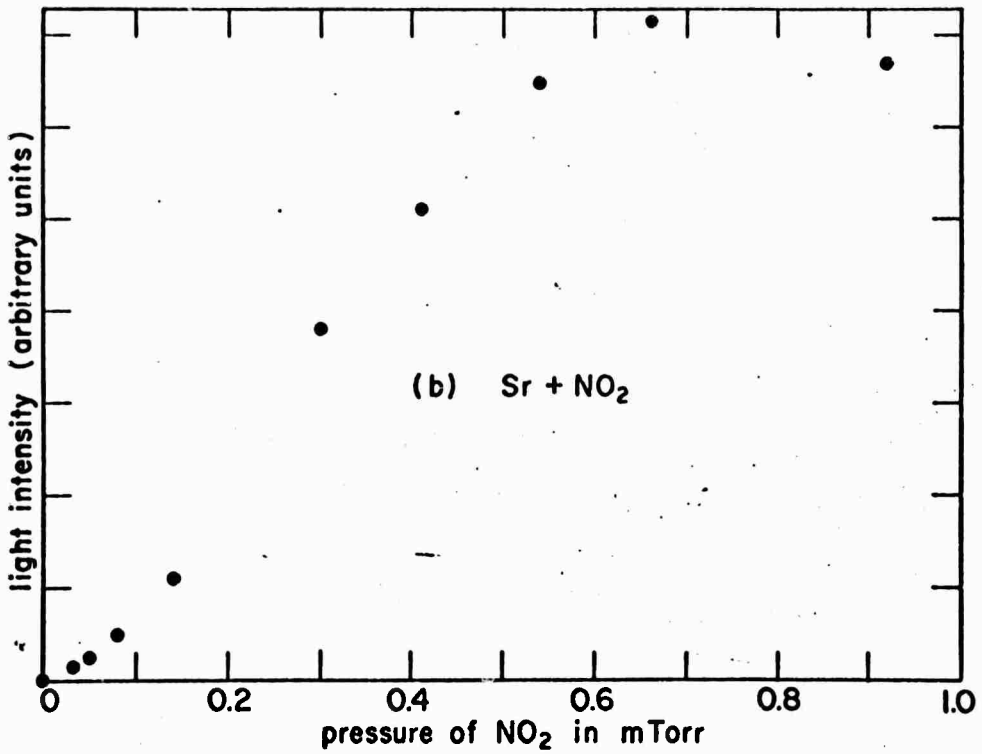
(b) Sr + NO_2
light intensity (arbitrary units)
0
0.2
0.4
0.6
0.8
1.0
pressure of NO_2 in mTorr

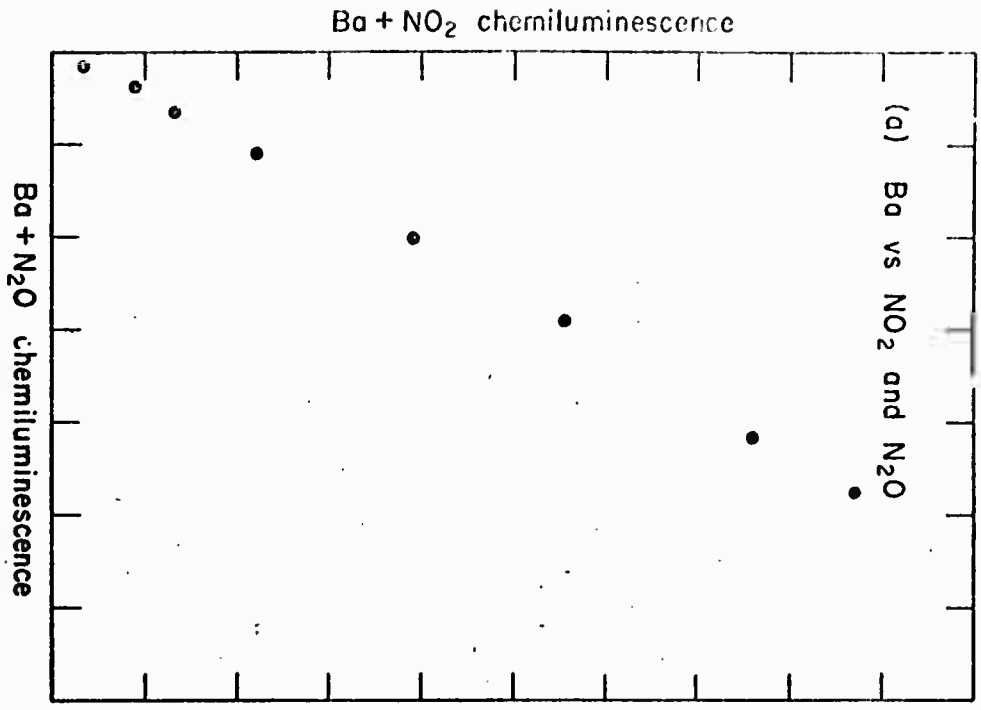
Ba + NO2 chemiluminescence
Ba + N2O chemiluminescence
(a) Ba vs NO2 and N2O

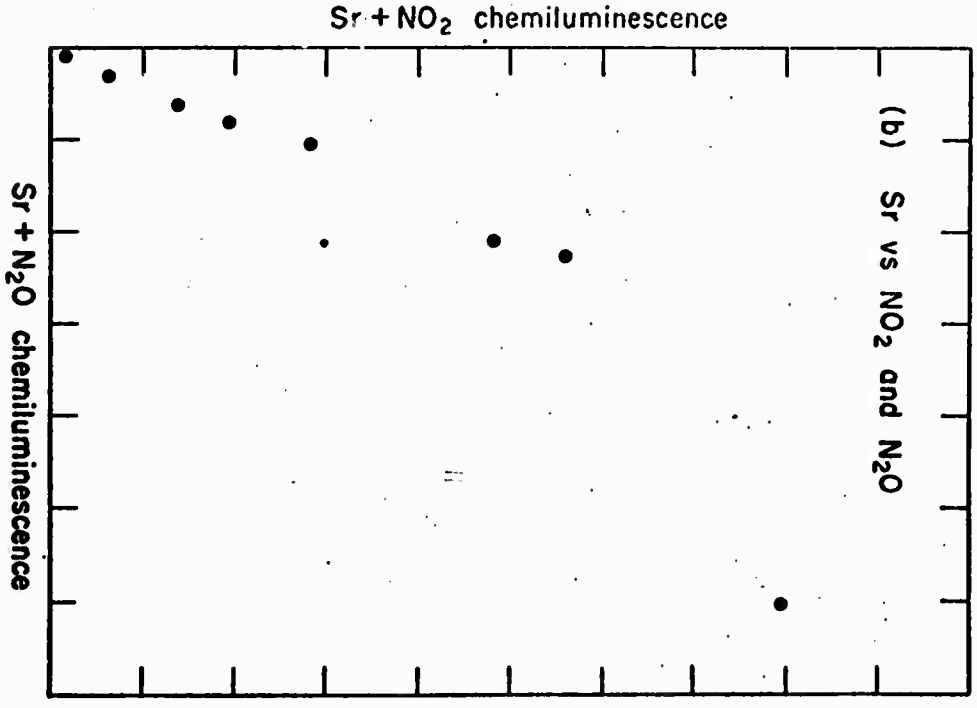
Sr + NO2 chemiluminescence
Sr + N2O chemiluminescence
(b) Sr vs NO2 and N2O

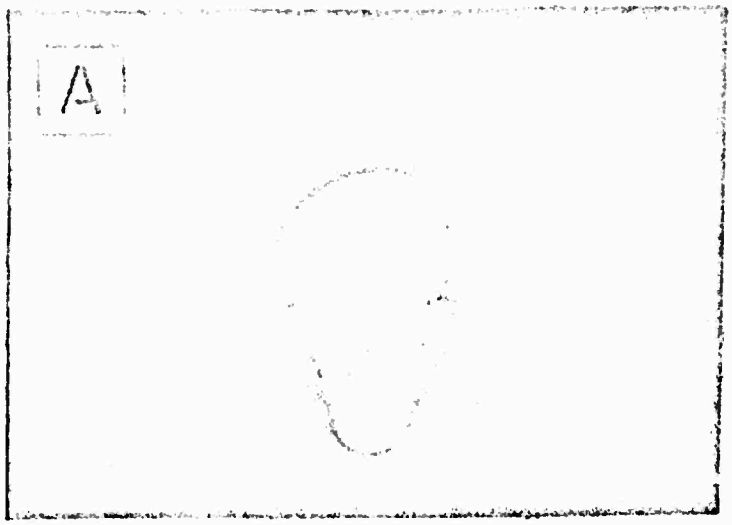

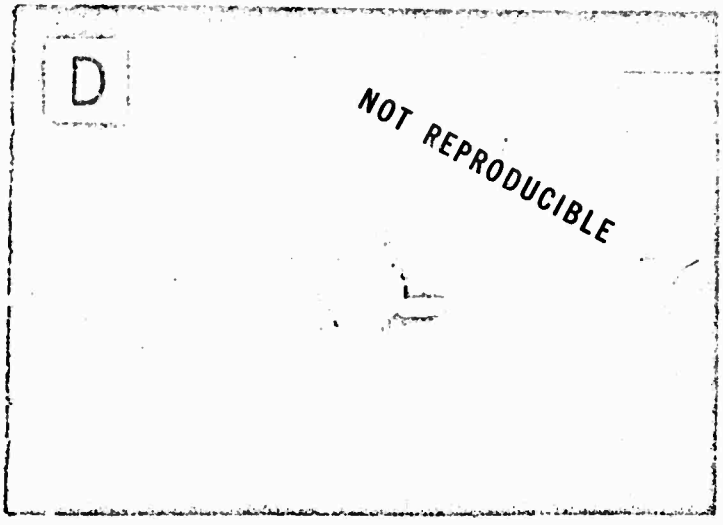

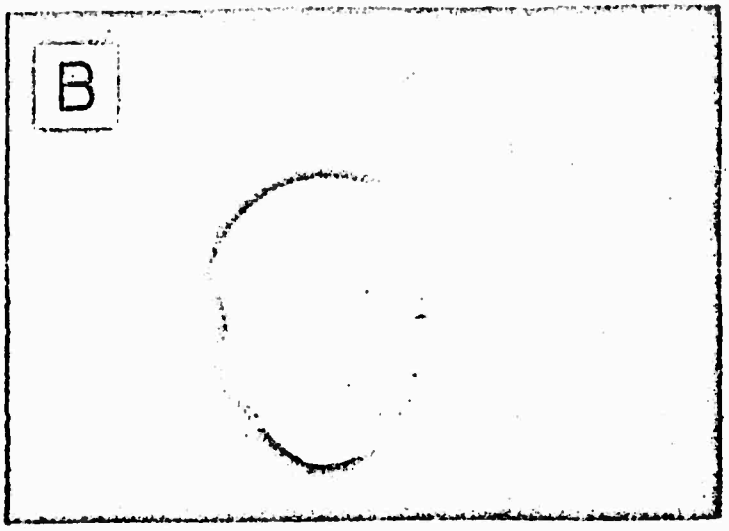

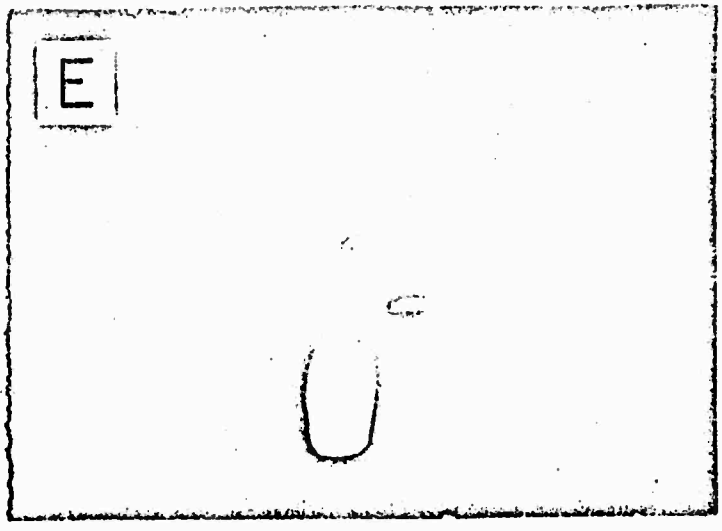

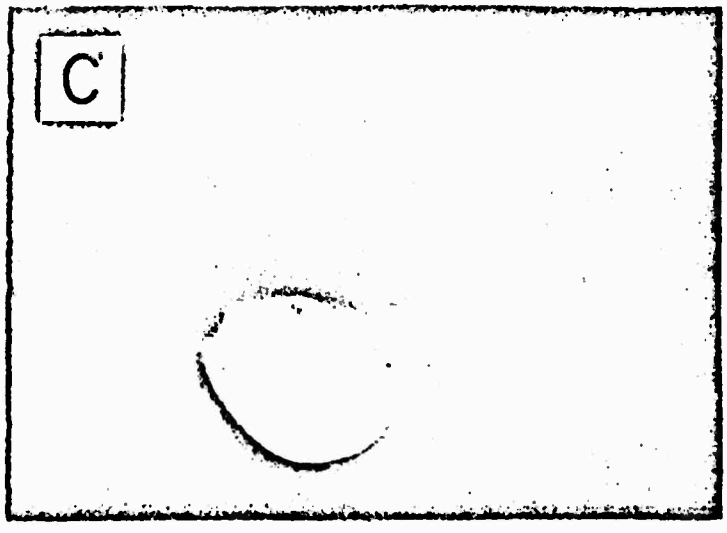

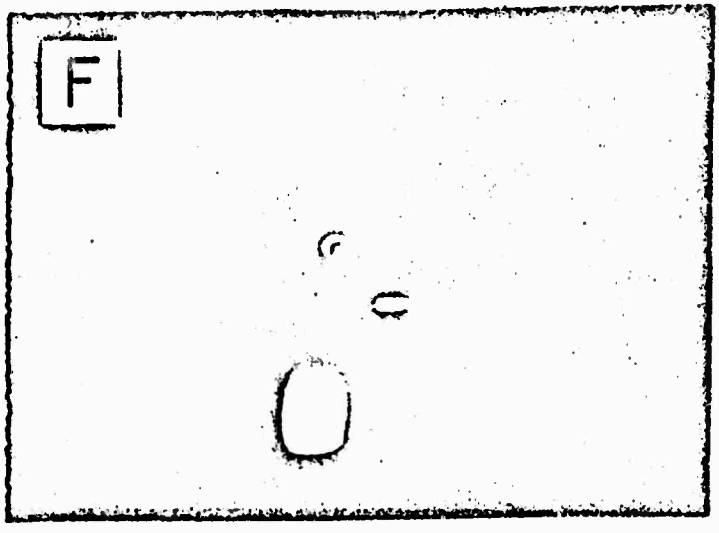

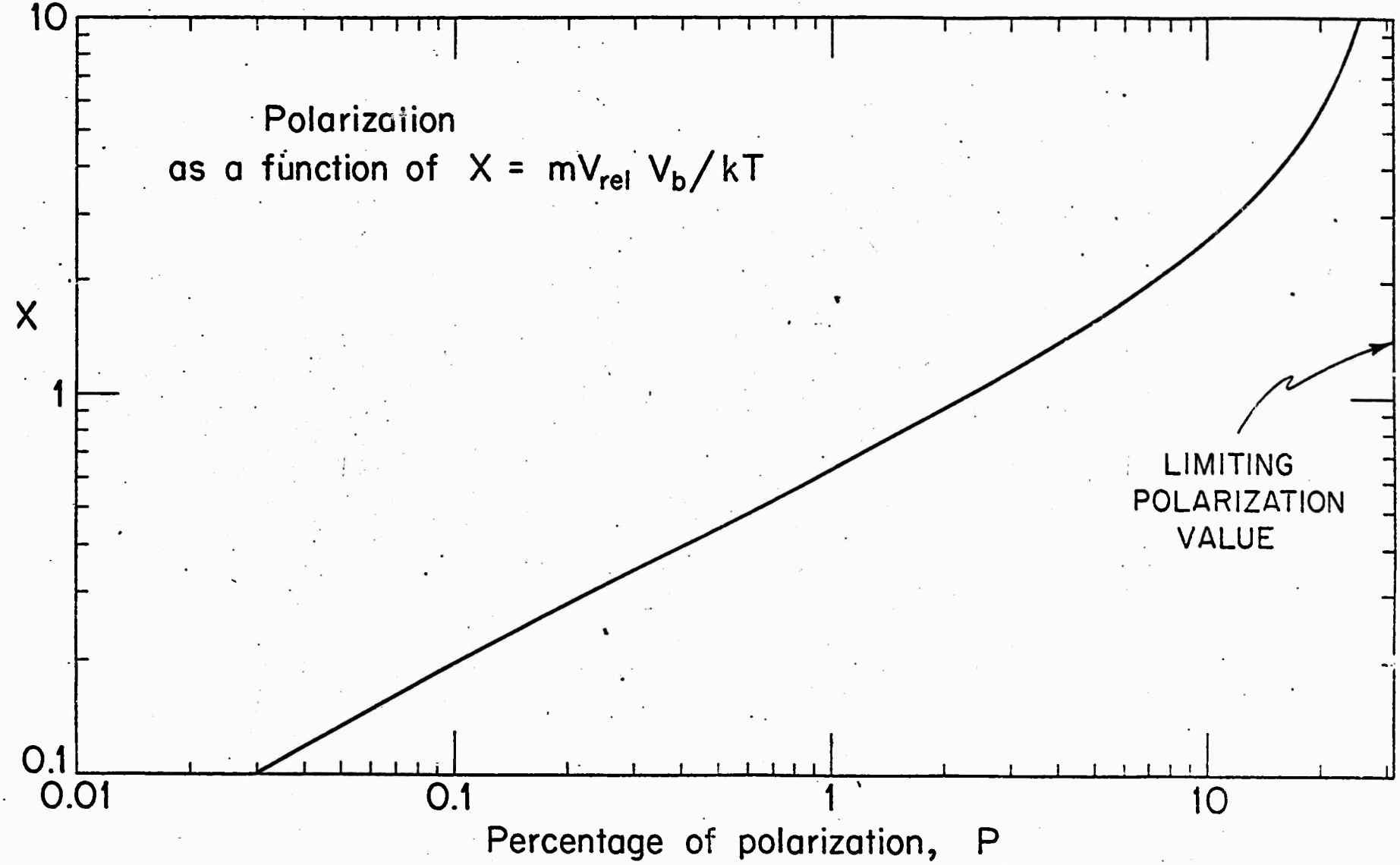
Polarization
as a function of X = mV_rel V_b / kT
X
10
1
0.1
0.01
0.1
1
10
Percentage of polarization, P
LIMITING
POLARIZATION
VALUE